

## Ultrafast chemistry in complex and confined systems

PARTHA DUTTA and KANKAN BHATTACHARYYA\*

Department of Physical Chemistry, Indian Association for the Cultivation of Science, Jadavpur,  
Kolkata 700 032, India  
e-mail: pckb@mahendra.iacs.res.in

MS received 15 December 2003

**Abstract.** Self-organized molecular assemblies play a crucial role in many natural and biological processes. Recent applications of ultrafast laser spectroscopy and computer simulations revealed that chemistry in a confined environment is fundamentally different from that in ordinary solutions. Many recent examples of slow dynamics in constrained environments and their biological implications are discussed.

**Keywords.** Organized assemblies; ultrafast laser spectroscopy; computer simulations.

### 1. Introduction

Weak molecular interactions play a central role in structure, function and dynamics of self-organized molecular assemblies. In an aqueous solution, self-assembly occurs because of the tendency of an amphiphilic molecule to hide the hydrophobic portion from bulk water and to expose the hydrophilic part (figure 1). The interplay between hydrophobic and hydrophilic interactions results in many binding processes (e.g. antigen–antibody, enzyme–substrate). Such a binding process is fundamental in molecular recognition and targeted drug delivery,<sup>1</sup> and has given rise to many emerging areas such as dynamic combinatorial chemistry,<sup>2</sup> and adaptive chemistry.<sup>3</sup>

In the last decade, application of ultrafast laser spectroscopy and large scale computer simulations has significantly improved our understanding of the primary steps of the ultrafast processes in organized assemblies. It has been demonstrated that chemistry in a self-organized assembly differs from that in a bulk liquid in a number of ways. First, confinement imposes considerable constraints on the free movement of the reactants and, hence, retards reactions which involve large amplitude motions (e.g. isomerization). Second, in a confined environment the static polarity of water is lower by a factor 3–5 and the solvation time is 100–1000 times slower<sup>4–8</sup> compared to bulk water.<sup>9–10</sup> The dramatic retardation of solvation dynamics causes insufficient and incom-

plete solvation of the polar transition state and, thus, markedly slows down polar reactions in a confined system. In this article, we give an overview of isomerization, slow solvation, and polar reactions in complex assemblies.

### 2. Photoisomerization

In the ground state of a molecule, *cis–trans* isomerization about an olefinic double bond is forbidden because of the involvement of a high energy barrier which is roughly equal to the  $\sigma$  bond energy. In the  $\pi\pi^*$  excited state, the  $\sigma$ -bond order becomes zero. Thus, in the excited state, isomerization involves no energy barrier and occurs freely. Such an interconversion of different rotamers via the excited state is known as photoisomerization. If the rotating group sweeps across a large volume of the solvent, the friction (viscosity) offered by the local environment profoundly influences the dynamics of isomerization.

It should be noted that the exact nature of structural change accompanying the isomerization process is different in different systems. In olefines or polyenes, isomerization involves rotation about a carbon–carbon double bond. In the case of triphenyl methyl (TPM) dyes (cresyl violet, malachite green etc.), the three phenyl rings undergo a propeller-like motion. The *trans*-azo-benzene molecule undergoes photoisomerization about the N–N double bond following a slightly different mechanism. In this case, the isomerization involves inversion in the  $S_1$  state

\*For correspondence

instead of rotation in the  $S_2$  state.<sup>11</sup> In 1985, Liu and co-workers proposed a new mechanism for the *cis-trans* isomerization process.<sup>12</sup> They suggested that *cis-trans* isomerization for a confined polyene such as the retinal chromophore in the visual pigment rhodopsin does not involve turning over half of the polyene, but instead involves translocation of a sin-

gle C-H unit by the simultaneously rotation of two connected single bonds and the double bond. Initially, this mechanism was called concerted twist at centre  $n$  (CT- $n$ ). Later this term has been replaced by a term locally popular as Hawai-Hula twist at centre  $n$  (HT- $n$ ). This process is volume conserving and, hence, does not depend strongly on solvent viscosity (friction).

The major importance of photoisomerization stems from the fact that many important proteins and drugs involve this process. The photophysical cycle of the visual pigment rhodopsin involves isomerization and hence isomerization is central in the vision process.<sup>13-14</sup> Most recently, it has been shown that photoisomerization plays a key role in two proteins, green fluorescent protein (GFP)<sup>15</sup> and photoactive yellow protein (PYP).<sup>16</sup> Owing to its intense fluorescence GFP is a very popular intrinsic probe for study of cell dynamics. In the denatured form, GFP is almost non-fluorescent ( $f_f < 10^{-3}$ ). The isolated chromophore of GFP dissolved in fluid solutions also displays negligible fluorescence intensity.<sup>17</sup> There has been several studies to elucidate the non-radiative pathway of GFP and thus to explain the origin of the intense fluorescence of GFP.

Recently, Meech and coworkers<sup>17</sup> reported that the fluorescence decay of the chromophore of GFP in alcohol displays a component of 1–3 ps and a faster component. The ultrashort decay of the fluorescence indicates a very fast non-radiative process. The 1–3 ps component is found to be weakly dependent on the solvent viscosity. The lack of significant viscosity dependence indicates that in this case the isomerization does not involve significant displacement of solvent molecules. Following Liu's model, it is suggested that HT- $n$  is the main non-radiative pathway in green fluorescent protein (GFP). The ultrafast HT- $n$  process readily occurs in solution resulting in very weak fluorescence and ultrashort lifetime. However, when the chromophore is surrounded by bulky protein chains in the protein GFP, HT- $n$  is prevented, giving rise to an intense fluorescence.<sup>17</sup> Most recently, ultrafast studies have shown that the important drug molecule cholchicine involves isomerization.<sup>18</sup>

The dynamics of *cis-trans* photoisomerization of a polyene depends on the viscosity of the medium.<sup>19</sup> At a very high viscosity, the rate of photoisomerization ( $k_{iso}$ ) is inversely proportional to bulk viscosity (Smoluchowski limit). The microviscosities of these assemblies may be determined from  $k_{iso}$ .<sup>20</sup>

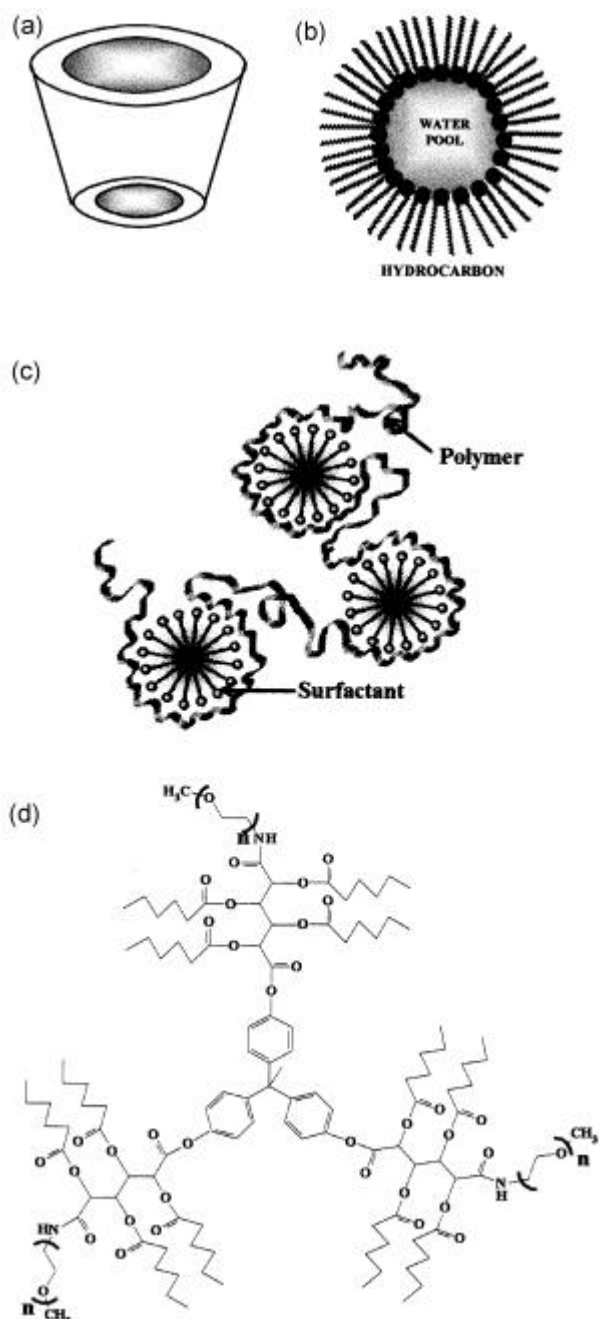


**Figure 1.** Structure of some organized assemblies. (a) cyclodextrin, (b) microemulsion, (c) polymer-surfactant aggregate and (d) amphiphilic star like macromolecule (ASM).

Organized assemblies hinder the isomerization process and cause an increase of the excited state lifetime of the rotamer which undergoes the isomerization. The rate of photoisomerization of stilbene in various organized assemblies is found to be slower compared to that in a homogeneous medium. Eisinger and co-workers studied isomerization dynamics of stilbene encapsulated in cyclodextrin cavities.<sup>21</sup> Cyclodextrins form supramolecular complexes with organic guest molecules and trap the guest with several solvent molecules (water and several other polar solvents). They are routinely used to increase the solubility of drugs in water and to release them at suitable targets. Fluorescence lifetime of *trans*-stilbene increases from 34 ps in aqueous methanol to 137 ps inside an  $\alpha$ -cyclodextrin ( $\alpha$ -CD) cavity.<sup>21</sup> This indicates that the isomerization of stilbene inside the  $\alpha$ -CD cavity is slower than in aqueous methanol. In  $\beta$ - or  $\gamma$ -CD, the fluorescence decays of *trans*-stilbene are biexponential with one component of 50 ps and another very slow component of several thousand picoseconds. The latter corresponds to a very rigid microenvironment where *cis*-*trans* isomerization is totally prevented.<sup>21</sup> It is proposed that in the small  $\alpha$ -CD cavity a major part of the stilbene molecule sticks out of the cavity and hence it undergoes isomerization though somewhat slowly. In  $\beta$ - or  $\gamma$ -CD the stilbene molecule is totally enclosed in the cavity (in 1:2 complexes) and as a result, the motion associated with isomerization is severely hindered.<sup>21</sup> The isomerization of methyl orange in cyclodextrin cavities is also found to depend on the cavity size and host-guest complexation ratio.<sup>22</sup> In NaY zeolite, in solvent-free condition, the lifetime of *trans*-stilbene is 52 ps compared to 66 ps in hexane and 32 ps in methanol.<sup>23</sup> However, the lifetime increases by a factor of 4 and 5 when NaY is saturated by either water or cyclohexane respectively. This is ascribed to the restriction of the motion of the probe due to the presence of solvent molecules inside the zeolite.<sup>23</sup>

Photoisomerization of a cyanine dye, merocyanine 540 (MC540) is retarded inside a micelle,<sup>24-25</sup> microemulsion<sup>24,26</sup> and protein.<sup>24</sup> The rate of photoisomerization of MC540 in water is 27 times faster than that in dioxane which is iso-viscous with water.<sup>24</sup> It is shown that the isomerization of MC540 involves an energy barrier which decreases with increase in solvent polarity.<sup>24</sup> The retardation of isomerization of MC540 in micelles and protein is predominantly due to the lower polarity of these sys-

tems compared to water.<sup>24</sup> The quantum yield of several other merocyanine dyes depends on polarity and viscosity of the medium and has been shown to report local properties of a protein.<sup>27</sup> The torsional motion of the triphenylmethane (TPM) dyes is significantly hindered in a protein resulting in a dramatic increase in the emission quantum yield and lifetime. Baptista and Indig reported a 1000-fold increase in the emission quantum yield and lifetime of TPM dyes on binding to a protein, bovine serum albumin (BSA).<sup>28</sup> Eisinger and co-workers studied photoisomerization at the air-water interface, using surface second harmonic generation.<sup>29-30</sup> For the rod-shaped molecule 3,3'-diethyloxadicyanin iodide, a major part of the probe is projected out in air and, as a result, isomerization at the air-water interface is found to be faster than that in bulk water.<sup>29</sup> However, the nearly planar molecule malachite green remains completely immersed in the surface layer and for this probe isomerization is slower at the air-water interface compared to bulk water.<sup>30</sup>

### 3. Solvation dynamics

Solvation refers to stabilization of a charged or dipolar solute by the collective reorientation of solvent dipoles. Solvation time is defined as the time required for the solvent reorganization following creation of the charge or the dipole. To study the solvation dynamics experimentally, one uses a solute whose dipole moment is nearly zero in the ground state but is very large in the excited state. In a solution of the non-polar solute in its ground state dissolved in a polar solvent, the solvent dipoles remain randomly arranged. When the solute is excited by an ultrashort light pulse, a dipole is created suddenly. Immediately after creation of the solute dipole, the solvent dipoles are randomly oriented and the energy of the system is high (figure 2). With increase in time, as the solvent dipoles reorient the energy of the solute dipole decreases and its fluorescence maximum gradually shifts to lower energy, i.e. towards longer wavelength. This is known as time dependent fluorescence Stokes shift (TDFSS). Evidently, at short wavelengths, the fluorescence corresponds to the unsolvated solute and exhibits decay. At long wavelengths, the fluorescence originates from the solvated species and a rise precedes the decay. The rise at a long wavelength corresponds to the formation of the solvated species and, hence, is a clear manifestation of solvation dynamics.

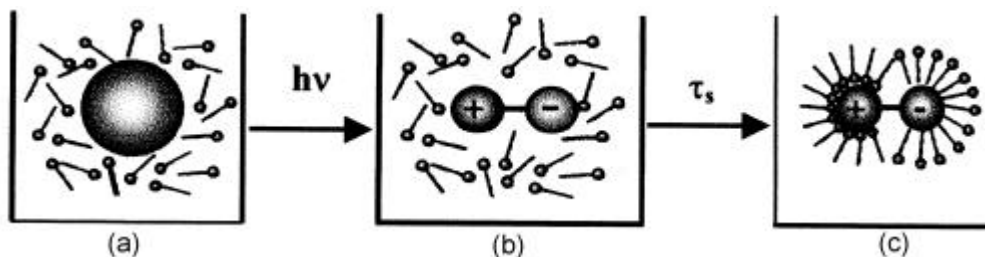


**Figure 2.** Solvation dynamics: Arrangement of solvent dipoles (match sticks) (a) before excitation of the solute and (b) immediately after creation of the dipole by the excitation of the solute. (c) Fully solvated solute dipole.

Solvation dynamics is monitored by the decay of the time correlation function  $C(t)$  which is defined as,

$$C(t) = \frac{E(t) - E(\infty)}{E(0) - E(\infty)}, \quad (1)$$

where  $E(0)$ ,  $E(t)$  and  $E(\infty)$  denote the observed emission energies of the system at time zero,  $t$  and infinity respectively. Obviously,  $E(0) > E(t) > E(\infty)$ . At  $t = 0$ , the value of  $C(t)$  is one and at  $t = \infty$  it is zero.

According to a continuum model, the solvation time ( $t_s$ ) is equal to  $(\epsilon_\infty/\epsilon_0)t_D$ , where  $\epsilon_\infty$  and  $\epsilon_0$  are respectively the high frequency and static dielectric constants of the solvent and  $t_D$  is the dielectric relaxation time.<sup>4,7,31</sup> For water,  $t_D$  is 8.3 ps, while  $\epsilon_\infty$  and  $\epsilon_0$  are respectively about 5 and 80. Thus according to the continuum theory the solvation time of water should be about 0.5 ps. Actual experiments also suggest that solvation dynamics in bulk water occurs in a less than one picosecond time scale. The longest component of decay of  $C(t)$  in bulk water is about 1 ps and a major part occurs in a time scale  $< 0.1$  ps.

Many recent experiments demonstrate that water molecules confined in many organized and biological assemblies exhibit a very slow component of solvation dynamics in 100–1000 ps time scale. It may be noted that in many organized assemblies, the dielectric relaxation time ( $t_D$ ) is about 10 ns.<sup>32–34</sup> The dielectric constant ( $\epsilon_0$ ) of confined water is close to that of alcohol (i.e. about 30).<sup>4–5,7</sup> If we assume that the high frequency dielectric constant ( $\epsilon_\infty$ ) in a supramolecular assembly is the same as that in water, according to the continuum model the solvation time is  $(5/30) \times 10$  ns or about 1600 ps. Thus the very long component of the solvation dynamics in 1000 ps

time scale may be attributed to slow dielectric relaxation.

To explain the slow component of dielectric relaxation and solvation dynamics, Nandi–Bagchi proposed a phenomenological model.<sup>35</sup> In this model, the so-called biological water i.e. water in the vicinity of a biological system is considered to be made up of two kinds of water molecules – bound and free. Bound water refers to those molecules which are attached to the biomolecule by one or two hydrogen bonds and are essentially immobilized. The free water molecules retain the hydrogen bond network in bulk water and exhibit bulk-like fast dynamics. Nandi–Bagchi showed that slow dielectric relaxation results from a dynamic equilibrium between bound and free water.<sup>35</sup> A water–biomolecule hydrogen bond is stronger than a water–water hydrogen bond. Thus, the bound water molecules are stabler than the free water molecules.<sup>35</sup> The slow component depends on the free energy difference ( $\Delta G^0$ ) between bound and free water molecules.<sup>35</sup> In the limit of very high binding energy,

$$t_{\text{slow}} \approx k_{\text{bf}}^{-1}, \quad (2)$$

where the rate of bound-to-free interconversion ( $k_{\text{bf}}$ ) is given by,

$$k_{\text{bf}} = (k_B T/h) \exp(-E_{\text{a,bf}}/RT). \quad (3)$$

The activation energy  $E_{\text{a,bf}}$  is a sum of the free energy difference of the bound and free water and the activation energy  $E_{\text{a,fb}}$  for free to bound interconversion.

More recently, many groups have carried out large-scale computer simulations on the solvation dynamics in organized assemblies. According to recent computer simulations at the surface of a micelle, the translation diffusion coefficient of water is not

too different from bulk water but the reorientation and solvation dynamics of water are slowed down significantly.<sup>36–40</sup> In the case of SDS micelle the translational diffusion coefficient of the interfacial water molecules in the first shell, second shell and third shell are in the ratio 0.6:0.8:1.<sup>40</sup> Thus, the difference in the translational diffusion coefficient between the first hydration shell of the micellar surface and the bulk water is not a significant one. The reasons behind the bulk-like diffusion may be as follows. First, for outward diffusion normal to the micellar surface, the water molecules become bulk-like just after travelling one water layer. Diffusion along the surface of the micelle where the water is enclosed in the first layer all the time may be much slower. Second, since the translational diffusion itself is a slow process, transient hydrogen bonding does not affect the slow translational diffusion significantly. We will discuss the results on slow reorientational and solvation dynamics later.

### 3.1 Solvation dynamics in supramolecular assemblies

**3.1a Cyclodextrins:** A supramolecule in which a solvation probe is confined along with several solvent molecules inside a cyclodextrin cavity (figure 1a) is perhaps the most well-defined example of a confined liquid. Fleming *et al*<sup>41</sup> studied solvation dynamics of water confined in a **g**-cyclodextrin cavity and detected three very slow components of 13 ps, 109 ps and 1200 ps. They ascribed the very slow component of solvation dynamics to three processes. First, the restricted motion of the highly confined water molecules; second, the motion of the guest probe molecule in and out of the cavity; and third, the fluctuations of the **g**-cyclodextrin ring.

Sen *et al*<sup>42</sup> studied solvation dynamics of a non-aqueous solvent, dimethylformamide in a **b**-cyclodextrin cavity. The dynamics of confined dimethylformamide molecules is found to be described by two slow components of 400 ps and 8000 ps.<sup>42</sup> This is substantially slower than the solvation (~1 ps) in bulk dimethylformamide.<sup>9</sup>

Nandi and Bagchi<sup>43</sup> ascribed the slow dynamics inside the cyclodextrin cavity to almost complete suppression of the translational modes of the trapped water molecules in the **g**-CD cavity.

**3.1b Micelles:** Micelles are spherical aggregates of surfactants with a ‘dry’ hydrocarbon core and a

polar peripheral shell which contains polar/ionic head groups, counter ions and water molecules. Solvation dynamics of the water molecules hydrogen-bonded to the polar head groups of a micelle exhibit a very slow component in the 100–1000 ps time scale. Most recently, solvation dynamics has been studied in bile salt micelles. The bile salts are natural amphiphiles which exhibit two critical micellar concentrations at ~ 10 mM (CMC<sub>1</sub>) and ~ 60 mM (CMC<sub>2</sub>). Above CMC<sub>1</sub>, bile salts form primary aggregates containing very few monomers with the hydrophilic groups pointing outwards.<sup>44</sup> Above CMC<sub>2</sub>, secondary aggregates are formed which resemble an elongated rod with a central hydrophilic core filled with water and the ions. The solvation dynamics of DCM in a secondary aggregate of sodium deoxycholate (NaDC) is found to be triexponential with components of 110 ps, 700 and 2750 ps.<sup>45</sup> These components are significantly slower than those in bulk water.

In order to develop a molecular picture of solvation dynamics in a micelle, many groups have carried out many large-scale computer simulations. Bagchi and Balasubramanian carried out fully atomistic molecular dynamics simulations on hydrogen bond dynamics,<sup>36</sup> solvation<sup>37–38</sup> and orientational dynamics<sup>39</sup> at the surface of a micelle, cesium pentadecafluorooctanoate (CsPFO). They detected a slow component of decay of the solvent correlation function  $C(t)$ . The decay of  $C(t)$  at the micellar surface<sup>37</sup> obtained by them may be fitted to a tri-exponential function having components, 1.6 ps, 4.3 ps and 30 ps. The ultrafast components (1.6 and 4.3 ps) detected in this simulation<sup>37</sup> are close to the ultrafast components of solvation dynamics detected in a recent femtosecond up-conversion study.<sup>46</sup> The lifetime of the hydrogen bond between a water molecule and the polar head group of a micelle is about 13 times slower than that of a water–water hydrogen bond and the activation barrier for interconversion of free-to-bound water in a micelle is 3.5 kcal/mol.<sup>36</sup> In a computer simulation Pal *et al*<sup>38</sup> found that the hydrogen bond energy of the interfacial water molecules which form one or two hydrogen bonded with the polar head groups of the micelles is about 13–14 kcal mol<sup>-1</sup>. This is about 7–8 kcal mol<sup>-1</sup> higher than the hydrogen bond energy between two water molecules in bulk water. Thus it appears that the rate-determining step in the micellar solvation is rupture of the hydrogen bond(s) between the water and the polar head groups. Most recently, Sen *et al*<sup>47</sup>

found experimentally that the activation energy of solvation in a micelle is  $9 \text{ kcal mol}^{-1}$ . This is consistent with the temperature-dependence predicted in a recent micellar simulation.<sup>38</sup>

In a molecular dynamics simulations on sodium dodecyl sulphate (SDS) micelle, Berkowitz and co-workers<sup>40</sup> found that about 60% of the interfacial water molecules are singly hydrogen bonded to the micelle, while 33% of them form two such hydrogen bonds and 7% of the interfacial water molecules do not form any hydrogen bond with the micelle. It was also found that the reorientational time correlation function for the dipoles of the water molecules within a 6-Å hydration layer exhibits a slow component of reorientational dynamics which is slower by one or two orders of magnitude than that in bulk water. They attributed the slow orientational motion next to the micellar surface to the locking of water molecules into certain configurations due to strong hydrogen bonding between the water molecule and the headgroup oxygen of the surfactant. It was also pointed out that the structural and dynamical properties of the water molecules in the second shell around the micelle are substantially different from those of bulk water and, beyond the second shell, water molecules are similar to bulk water.<sup>40</sup>

**3.1c Reverse micelles and microemulsions:** In a microemulsion, the water molecules exist as nanometre-sized droplets, called a 'water pool.' The water pool is surrounded by a layer of surfactant molecules whose polar head groups point inward (figure 1b).<sup>5,7-8,48</sup> The water pool in a microemulsion is an elegant model of confined water molecules. For the surfactant, the AOT (sodium dioctyl sulphosuccinate) radius of the water pool is approximately  $2w_0$  (Å) where  $w_0$  denotes the water to surfactant molar ratio. In a water pool with  $w_0 > 10$ , solvation dynamics of water exhibits a component in 100–1000 ps time scale which is slower by three orders of magnitude compared to bulk water.<sup>5,7</sup>

Most recently, it is proposed that self-diffusion of a solvation probe from the water-surfactant interface to the core of the water pool may be a source of the ultraslow component of solvation. It has been reported that the full width at half maximum (FWHM,  $\Gamma$ ) of the TRES changes appreciably with time. It may be noted that in bulk water and in many liquids the width ( $\Gamma$ ) changes by a small amount (10–20%) with time.<sup>31</sup> The major source of the width of the emission spectra is the fluctuation in the local sol-

vent environment.<sup>31</sup> In a simple liquid the variation of the local solvent environment is small and hence the variation of  $\Gamma$  with time is small. In the microemulsions  $\Gamma$  exhibits a dramatic decrease with increase in time by over 50%.<sup>49</sup> The time-dependence of  $\Gamma$  has been ascribed to self-diffusion of the probe (DCM) as follows.

DCM is insoluble in water. On electronic excitation, DCM becomes more polar and presumably more soluble in the core of the water pool. As a result, after excitation it may migrate from the AOT interface towards a more polar region of the water pool. Translational diffusion coefficients ( $D$ ) of several organic probes in many organized assemblies have been obtained from fluorescence anisotropy decay.<sup>50</sup> In the organized assemblies  $D$  of several organic probes is found to be around  $5 \times 10^{-10} \text{ m}^2 \text{ s}^{-1}$  which is close to those in bulk water.<sup>50</sup> Thus according to the relation  $\langle z^2 \rangle = 2Dt$ , the DCM molecule travels 1 nm per ns inside the microemulsion.

At  $t = 0$ , DCM molecules near AOT experience a large variation in the solvent environments. Note, there are about 4 water layers of thickness  $\approx 0.3 \text{ nm}$  over the length, 1.25 nm, of the DCM molecule. All such DCM molecules are excited simultaneously. Due to the superposition of the emission spectra of DCM in different environments at short intervals of time the spectral width is very large. Following electronic excitation, DCM moves away from the AOT interface to the water pool. Thus over a long time, the emission spectrum originates from the DCM molecules at a relatively large distance from AOT. This corresponds to a more uniform environment and hence, leads to a smaller spectral width. Thus the decay of  $\Gamma$  with time may be ascribed to self-diffusion of the probe inside the water pool. It is likely that in the solvation dynamics in the water pool the rate-determining step is the diffusion of the probe from the AOT interface where the bound water molecules are immobilized to a region quite distant from the AOT molecules where water molecules are quite free and exhibit ultrafast dynamics. Thus the solvation dynamics in the water pool is controlled by the diffusion of the probe and is similar to the decay of  $\Gamma$ . In summary, the slow components (100–1000 ps) in the decay characteristics of  $\Gamma(t)$  and  $C(t)$  of DCM in a water pool arises from self-diffusion of the probe.<sup>49</sup>

However, in the case of aggregates of Na-cholate in bulk water  $\Gamma$  does not change much with time and the time-dependence of  $\Gamma$  is similar to that in simple

liquids.<sup>49</sup> Thus self-diffusion is not a universal mechanism of the slow solvation dynamics. In the case of Na-cholate aggregates, the central water filled channel is very thin and about 5 nm long.<sup>44</sup> It appears that the probe (DCM) remains in a uniform environment within the channel during its entire life time.

For a microemulsion, Faeder and Ladanyi<sup>51</sup> carried out a simulation up to 10 ps and did not detect the slow dynamics in 100–1000 ps time scale. Senapati and Chandra<sup>52</sup> showed that the dielectric constant and solvation time inside a microemulsion is lower than that in bulk water by less than one order of magnitude. According to Senapati and Berkowitz,<sup>53</sup> the earlier simulations of Ladanyi group did not detect the slow dynamics because the latter modelled the interior of the water pool as rigid. Berkowitz and coworkers carried out MD simulations in the water pool of phosphate fluorosurfactant based reverse micelles in supercritical carbon dioxide.<sup>53</sup> They found that the water molecules in the first solvation shell of the headgroup are strongly bonded to the surfactant headgroups and thus disrupt the water–water tetrahedral hydrogen-bonded network. They specified the water molecules in the first hydration shell as ‘bound’ and the region as ‘region I’. The translational mobility of the water molecules in ‘region I’ is reduced by a factor of six compared to bulk water. 25 water molecules are found to stay in ‘region I’ through out a time period of 1.8 ns. Compared to ‘region I’, the water molecules in ‘region II’ are more mobile and hence, are called ‘free’ or ‘diffuse’. 18 water molecules stay in ‘region II’ for a time period of 160 ps. In ‘region III’, 15 water molecules stay for 20 ps. Thus, this is the most mobile region and the water molecules in ‘region III’ are bulk-like. The simulations reveal that 50% of the first shell water molecule form two surfactant to water hydrogen bonds and 40% of them form single hydrogen bond to surfactant oxygen. The average orientational correlation times are 396, 41, 3.8 and 3.2 ps for ‘region I’, ‘region II’, ‘region III’ and bulk water respectively.<sup>53</sup> The long component of the reorientational motion is 1700 ps for ‘region I’. Thus, the slow component of the reorientational relaxation of the water molecules in the first solvation shell is slowed down by three orders of magnitude compared to bulk water. This indicates that the water-headgroup hydrogen bond formation is the most important factor in the slow dynamics in restricted environment.

### 3.1d Polymer and polymer–surfactant aggregates:

Structure of a polymer in a solution depends on the solvent. In a ‘good’ solvent, the polymer remains in an extended form with a large end-to-end distance. In a ‘bad’ solvent, the polymer exposes only a part of itself which displays an attractive interaction towards the solvent. Thus in a ‘bad’ solvent the polymer assumes a hypercoiled form with a relatively small end-to-end distance. Water being highly polar, is usually a ‘bad’ solvent for many polymers consisting of non-polar or hydrophobic units. In a dilute solution of a polymer, individual polymers are well separated and interaction or entanglement of different polymer chains may be neglected. In such a situation the polymer chain remains self-entangled, i.e. different parts of the same polymer molecule interact or entangle with each other. At a concentration above the so-called cross-over value  $C^*$  (overlapping concentration), polymer chains of different polymer molecules become entangled and form a pseudo-network. The value of  $C^*$  is given by<sup>54</sup>

$$C^* = \frac{3N_s}{4p\langle R_g^2 \rangle^{3/2}}, \quad (4)$$

where,  $N_s$  is number of polymer segments and  $\langle R_g^2 \rangle$  is the unperturbed mean square radius of gyration of the polymer. The unperturbed radius of gyration ( $R_g$ ) is  $(\langle R_0^2 \rangle / 6)^{1/2}$ , where  $\langle R_0^2 \rangle$  is the mean square end-to-end distance of the polymer.

The highly hydrophobic polymer or protein molecules may be solubilized in water is through supra-molecular assembly of polymer and surfactants.<sup>1</sup> For instance, the protein zein is insoluble in water.<sup>55</sup> But, in the presence of a surfactant sodium dodecyl sulphate (SDS), the protein becomes soluble in water. It is proposed that in such a polymer–surfactant aggregate, the polymer chain becomes decorated with micellar aggregates (figure 1c).<sup>55–60</sup> Several authors have described such an aggregate as a ‘necklace’ with the spherical micelles as (‘beads’) and polymer chains as the ‘thread.’ Such an aggregate is formed at a concentration of the surfactant, called critical association concentration (CAC) which is often significantly lower than the critical micellar concentration (CMC) of the surfactant. In a polymer–surfactant aggregate, the polymer segments reduce two unfavorable interactions in a surfactant aggregate (micelle) viz., electrostatic repulsion among the head groups and residual contact of the first few pe-

ripheral carbon atoms of the hydrocarbon chains with water. Thus, fewer number of surfactant molecules (aggregation number) are required for the formation of the micelles in the presence of a polymer.<sup>56–60</sup> Lissi *et al*<sup>60</sup> reported that the aggregation number of SDS is  $\sim 35$  and  $\sim 30$  in the presence of polyethylene glycol (PEG) and polyvinylpyrrolidone (PVP) respectively, while in bulk water the aggregation number of SDS is 62.<sup>61</sup>

In a recent photon correlation study,<sup>56</sup> it has been reported that in the absence of the polymer at a concentration above CMC ( $\sim 8$  mM), the hydrodynamic diameter ( $d_h$ ) of SDS micelles is  $\sim 5$  nm. However, in the presence of PVP ( $\sim 3$  mg/mL) at a SDS concentration only 0.3 mM (CAC) very large aggregates ( $d_h \sim 12$  nm for PVP with molecular weight,  $M_w = 5 \times 10^4$  Da and  $d_h \sim 35$  nm for PVP with,  $M_w = 10^6$  Da) are formed.<sup>56</sup>

The solvation dynamics in a polymer–surfactant aggregate is found to be appreciably slower than that in a micelle or in an aqueous solution of the polymer.<sup>57–59</sup> Solvation dynamics of TNS in PVP–SDS aggregate is described by two components, 300 ps and 2500 ps.<sup>57</sup> In contrast, solvation dynamics of TNS occurs in  $< 50$  ps in SDS micelles while in an aqueous solution of PVP the solvation dynamics is described by a major (85%) component of 60 ps.<sup>57</sup> The slower solvation dynamics in PVP–SDS aggregate compared to the polymer PVP alone or SDS alone indicates severe restrictions on the mobility of the water molecule squeezed in between the polymer chains and the micellar (SDS) surface.<sup>57</sup>

There is considerable recent interest in synthesizing polymers with tailor-made structures suitable for drug delivery.<sup>1</sup> Since the biological system is aqueous, it is extremely important to develop water-soluble polymers. Recently, a large number of polymers have been developed which have a hydrophobic core and a hydrophilic peripheral shell.<sup>62</sup> In this case, one single polymer molecule resembles a surfactant aggregate (micelle). Such a polymer is called amphiphilic star-like macromolecule (ASM, figure 1d). They encapsulate highly hydrophobic drug molecules and thus solubilize them in water. Such a system has potential applications in targeted drug delivery.

Castner *et al*<sup>62</sup> studied solvation dynamics in aqueous solution of an amphiphilic star-like macromolecule (ASM) which consists of a hydrophobic core and a peripheral hydrophilic shell. The solvation dynamics in ASM is described by an ultrafast

component of 0.95 ps (44%) and two very slow components of 361 ps (19%) and 3962 ps (37%).<sup>62</sup>

**3.1e Proteins:** Water molecules at the surface of a protein govern molecular recognition (i.e. highly specific hydrophobic binding of a protein).<sup>32–34,63–66</sup> It is obviously of fundamental importance to elucidate how the hydration layer controls the structure, dynamics and function of a protein. Early studies on the dynamics of the water at the surface of a protein employed dielectric relaxation.<sup>32–34</sup> These studies reveal that while dielectric relaxation in bulk water is 8 ps, protein-bound water exhibits a thousand-fold slower component in the time scale of tens of nanoseconds. NMR studies also indicated that the residence time of water at the protein surface is on the order of 100 ps.<sup>65–66</sup> In the early nineties, there were several studies using phase modulation technique on solvation dynamics in protein both in the water pool of a microemulsion<sup>67</sup> and in bulk water.<sup>68</sup> They used both the single tryptophan residue as an intrinsic probe<sup>67</sup> and a non-covalent extrinsic probe.<sup>68</sup> These studies reveal a nanosecond component of solvation dynamics.

Since the late nineties, several groups applied ultrafast laser spectroscopy to study solvation dynamics directly in a protein. Fleming *et al*<sup>69</sup> studied dynamics of a non-covalent probe, eosin in the hydration layer of a protein (lysozyme) using the three-photon echo peak shift. They detected a very long component of 530 ps which is absent for free eosin in bulk water. This demonstrates that the water molecules in the immediate vicinity of the protein are highly constrained. Using time-dependent fluorescence Stokes shift, Pal *et al*<sup>70</sup> studied solvation dynamics of a non-covalent probe (DCM) bound to human serum albumin (HSA).<sup>70</sup> They detected two components of 600 ps (25%) and 10,000 ps (75%).<sup>70</sup> The 600 ps component is consistent with the 530 ps component obtained earlier by Fleming and co-workers and is consistent with an analytical theoretical model.<sup>35</sup> Very recently a new mechanism has been proposed to explain the origin of the very long 10,000 ps component.<sup>71</sup> The overall tumbling time ( $t_M$ ) of a protein is given by  $\hbar V/k_B T$  and is usually very long. For HSA ( $8 \times 8 \times 3$  nm),  $t_M$  is 25 ns. When HSA is encapsulated in a lipid (DMPC) vesicle the protein molecules cannot rotate individually. The diameter of DMPC vesicle is 30 nm and the corresponding  $t_M$  is so slow (3500 ns) that one may neglect it. It is observed that when the overall tum-



bling of the HSA molecule is suppressed by entrapping the protein in DMPC vesicle the 10,000 ps component vanishes. Thus the 10,000 ps is ascribed to the overall tumbling of the protein.<sup>71</sup>

Very recently, several groups studied solvation dynamics at a specific location of a protein using covalently attached probe and intrinsic probe, tryptophan.<sup>72–73</sup> Zewail *et al* reported that solvation dynamics of the intrinsic probe, tryptophan occurs in <1.1 ps in bulk water time scale while a long component of 38 ps is detected in a protein, Subtilisin Carlsberg (SC).<sup>72</sup> Mandal *et al*<sup>73</sup> attached a solvation probe covalently to a sulphhydryl group of the cysteine residue of glutaminyl RNA synthetase (GlnRS).<sup>73</sup> The sulphhydryl group is located at such a distance that about half (5 Å) of probe is buried inside the protein. They observed two components of 40 and 580 ps with an average solvation time of 120 ps.<sup>73</sup>

Most recently, several groups have reported on solvation dynamics in non-native states of a protein. Zewail *et al*<sup>74</sup> studied solvation dynamics in a protein,  $\alpha$ -chymotrypsin denatured by acid and found that the solvation dynamics in the denatured state is slower than that in the native state of the protein. They also found the same trend of solvation dynamics for the sweet protein, monellin, denatured by guanidine hydrochloride.<sup>75</sup> Bagchi and co-workers<sup>6</sup> explained the slow dynamics in the denatured state of monellin in terms of Rouse chain dynamics for a homopolymer and concluded that in the denatured state relaxation dynamics of protein spans 3 orders of magnitude. Dutta *et al*<sup>76</sup> studied solvation dynamics of coumarin 153 (C153) in a protein, lysozyme, denatured by SDS and dithiothreitol and found that solvation dynamics in the denatured protein is slower than that in the native state. The slow dynamics in the denatured protein is attributed to the polymer chain dynamics and the exchange of bound and free water.<sup>76</sup> Sen *et al*<sup>77</sup> studied solvation dynamics in a protein-folding intermediate, the molten globule state. In the molten globule state of a protein, glutaminyl-tRNA synthetase (GlnRS), for both covalent and non-covalent probes, the solvation times (250 and 400 ps respectively) are close whereas the solvation time of the non-covalent probe in the native state (1400 ps) is 12 times longer. The difference in solvation time in the native state of the protein is ascribed to different locations of the probes.<sup>77</sup>

Mukherjee *et al*<sup>78</sup> showed that though addition of small amount (80  $\mu$ M) of SDS keeps the structure of HSA intact, solvation dynamics of TNS in the HSA-

SDS aggregate is faster than that in HSA in bulk water. This is attributed to the displacement of the slow water molecules bound to the protein by SDS.<sup>78</sup>

3.1f *DNA*: Brauns *et al*<sup>79</sup> attached a solvation probe, coumarin 102 (C102), covalently to the deoxyribose moiety of DNA double-helix such that it replaced a normal base pair. They detected logarithmic relaxation times over three decades (40 ps–40 ns) indicating a complex relaxation among a large number of conformational substates.<sup>79</sup> Zewail and co-workers detected a ~10 ps component of solvation dynamics of water in the minor groove of DNA using 2-aminopurine as an intrinsic probe and a minor groove binding non-covalent probe, pentamidine.<sup>80</sup>

3.1g *Sol-gel glass*: Optical Kerr effect studies on various liquids confined in a sol-gel glass reveal a major bulk-like component and an additional component which is nearly 4 times slower.<sup>81</sup> In a sol-gel glass with 10 Å pores, the average solvation time of trapped water molecules is found to be 220 ps.<sup>82</sup> This is about 200 times slower than that in bulk water. The average solvation time of ethanol in bulk is 12.5 ps while it is 18.6 ps in a sol-gel glass with 75 Å pores and 35.9 ps in 50 Å pores.<sup>83</sup>

Very recently, Halder *et al*<sup>84</sup> studied solvation dynamics in an ormosil (i.e. a sol-gel glass containing entrapped organic guests). In the presence of dimyristoyl-phosphatidylcholine (DMPC) in the sol-gel glass, solvation dynamics of coumarin 480 (C480) is about 2.3 times slower than that in its absence.<sup>84</sup> The solvation dynamics inside the DMPC entrapped sol-gel is about 14 times faster than that in DMPC vesicles in bulk solution. This suggests that the liposomes are ruptured inside the sol-gel matrix.<sup>84</sup>

#### 4. Effect of slow solvation on polar reactions in organized assemblies

Solvation facilitates a polar reaction by reducing the activation energy barrier and stabilizing the product by differential stabilization of the transition state and the product with respect to the reactant. The slow solvation dynamics in organized assemblies causes marked reduction of many polar reactions, e.g. twisted intramolecular charge transfer (TICT),<sup>85–89</sup> excited state intermolecular proton transfer (ESPT)<sup>90–96</sup> and intermolecular electron transfer.<sup>97–100</sup>

About a decade ago Nag *et al*<sup>85–86</sup> reported that TICT process of dimethylamino-benzonitrile inside a cyclodextrin cavity depends markedly on the cavity size.<sup>85–86</sup> In the small **a**-CD, TICT is quite fast as a major part of the DMABN molecule sticks out. In a bigger **b**- or **g**-CD cavity, the entire DMABN molecule is enclosed and TICT is severely inhibited because of reduced polarity, slower solvation and restriction imposed on the twisting motion.<sup>87</sup> This results in a dramatic enhancement of the ‘non-polar’ emission of DMABN.<sup>86–87</sup> 1-(2-Naphthyl)-2-ethenyl-(2-benzothazolium) iodide (1,2-NEB) exhibits a twisting motion along the central C–C double bond which may be prevented in the nanocavity of cyclodextrin.<sup>89</sup> In the smaller **b**-CD cavity, *trans*-1,2-NEB cannot undergo twisting and intramolecular charge-transfer (ICT) and exhibits a lifetime of a few picoseconds. However, in the larger **g**-CD, *trans*-1,2-NEB has enough room to undergo twisting and ICT. Thus, in **g**-CD, the *cis* isomer results from the twisting and ICT and a nanosecond lifetime of the *cis* isomer is observed. Thus, the size of the cyclodextrin cavity controls occurrence of the *trans*-*cis* isomerization process.<sup>89</sup>

1-Naphthol is a weak base in the ground state ( $pK_a = 9.5$ ). In the excited state, 1-naphthol behaves as a strong acid ( $pK_a^* \approx 0.5$ ) and readily donates a proton to bulk water in 35 ps.<sup>90–92</sup> The essential condition for ESPT of 1-naphthol is adequate solvation of the anion and the proton. It is observed that in a supersonic jet ESPT of 1-naphthol occurs in a water cluster only if there are at least 30 water molecules in the cluster.<sup>91</sup> Methanol cannot solvate 1-naphthol and the anion because of steric hindrance. Consequently, ESPT of 1-naphthol does not occur either in a cluster with methanol in supersonic jet or in a liquid solution in methanol.<sup>91</sup>

Dynamics of ESPT of 1-naphthol is monitored by the decay of the emission from the neutral form (at 360 nm) and the rise of the anion emission (at 460 nm). The slow and inadequate solvation in an organized assembly results in a marked retardation of the ESPT process of 1-naphthol in the water pool of a microemulsion,<sup>92</sup> in cyclodextrin cavity,<sup>93</sup> micelle,<sup>94</sup> and in a polymer–surfactant aggregate.<sup>95</sup> Organero and Douhal studied excited state intramolecular proton transfer (ESIPT) of 1-hydroxy-2-acetonaphthone (HAN).<sup>96</sup> They reported significant retardation of the ESIPT process of HAN inside the **a**-CD cavity. This results in enhancement of fluorescence intensity and life time of the enol emission of HAN.<sup>96</sup>

The intermolecular electron transfer between a donor and an acceptor has been observed to be markedly retarded in a micelle.<sup>97–100</sup> Most recently, it is reported that intermolecular electron transfer in a micelle displays Marcus-inverted behaviour.<sup>100</sup>

## 5. Conclusion and future outlook

The recent applications of ultrafast spectroscopy and large scale computer simulations have provided molecular pictures of dynamics in biological assemblies in unprecedented detail. This has considerably improved our understanding of chemistry in a confined environment. The most important discovery is undoubtedly the slow component of solvation dynamics. At least four different mechanisms have been suggested to explain the surprisingly slow component of solvation dynamics. We are beginning to understand the biological implication of the slow solvation dynamics. This field has grown very rapidly in the last 5 years. Further studies in this area may ultimately explain biology in chemical terms and, with this end in view, this will remain a frontier area of research for quite sometime.

## Acknowledgements

Thanks are due to Council of Scientific and Industrial Research (CSIR), New Delhi and Department of Science and Technology (DST), Government of India for generous research grants. PD thanks CSIR for a fellowship. KB thanks Professor B Bagchi of the Indian Institute of Science, Bangalore for many stimulating discussions.

## References

1. Muller A and O'Brien D F 2002 *Chem. Rev.* **102** 727
2. Nitschke J R and Lehn J-M 2003 *Proc. Natl. Acad. Sci. (USA)* **100** 11970
3. Fernandez-Lopez S, Kim H-S, Choi E C, Delgado M, Granja J R, Khasanov A, Kraehenbuehl K, Long G, Weinberger D A, Wilcoxon K M and Ghadiri M R 2001 *Nature (London)* **412** 452
4. Bagchi B 2003 *Annu. Rep. Prog. Chem.* **C99** 127
5. Bhattacharyya K 2003 *Acc. Chem. Res.* **35** 95
6. Pal S K, Peon J, Bagchi B and Zewail A H 2002 *J. Phys. Chem.* **B106** 12376
7. Nandi N, Bhattacharyya K and Bagchi B 2000 *Chem. Rev.* **100** 2013
8. Levinger N E 2000 *Curr. Opin. Colloid. Interface Science* **5** 118

9. Jimenez R, Fleming G R, Kumar P V and Maroncelli M 1994 *Nature (London)* **369** 471
10. Nandi N, Roy S and Bagchi B 1995 *J. Chem. Phys.* **102** 1390
11. Fujino T, Arzhantsev S Y and Tahara T 2001 *J. Phys. Chem.* **A105** 8123
12. Liu R S H 2001 *Acc. Chem. Res.* **34** 555
13. Kim J E, McCamant W, Zhu L and Mathies R A 2001 *J. Phys. Chem.* **B105** 1240
14. Ruhman S, Hou B, Friedman N, Ottolenghi M and Sheves M 2002 *J. Am. Chem. Soc.* **124** 8854
15. Zimmer M 2002 *Chem. Rev.* **102** 759
16. Groot M L, van Wilderen L J G W, Larsen D S, van der Horst M A, van Stokkum I H M, Hellingwerf K J and van Grondelle R 2003 *Biochemistry* **42** 10054
17. Mandal D, Tahara T, Webber N M and Meech S R 2002 *Chem. Phys. Lett.* **358** 495
18. Bussotti L, Cacelli I, D'Auria M, Foggi P, Lesina G, Silvani A and Villani V 2003 *J. Phys. Chem.* **A107** 9079
19. Waldeck D H 1991 *Chem. Rev.* **91** 415
20. Pal S K, Datta A, Mandal D and Bhattacharyya K 1998 *Chem. Phys. Lett.* **288** 793
21. Duvencek G L, Sitzmann E V, Eisinger K B and Turro N J 1989 *J. Phys. Chem.* **93** 7166
22. Takei M, Yui H, Hirose Y and Sawada T 2001 *J. Phys. Chem.* **A105** 11395
23. Ellison E H and Thomas J K 2001 *J. Phys. Chem.* **B105** 2757
24. Mandal D, Pal S K, Sukul D and Bhattacharyya K 1999 *J. Phys. Chem.* **A103** 8156
25. Quitevis E L, Marcus A H and Fayer M D 1993 *J. Phys. Chem.* **97** 5762
26. Benniston A C, Matousek P, McCulloch I E, Parker A W and Towrie M 2003 *J. Phys. Chem.* **A107** 4347
27. Touthkine A, Kraynov V and Hahn K 2003 *J. Am. Chem. Soc.* **125** 4132
28. Baptista M S and Indig J L 1998 *J. Phys. Chem.* **B102** 4678
29. Sitzmann E V and Eisinger K B 1988 *J. Phys. Chem.* **92** 4579
30. Shi X, Borguet E, Tarnovsky A N and Eisinger K B 1996 *Chem. Phys.* **205** 167
31. Maroncelli M 1993 *J. Mol. Liq.* **57** 1
32. Grant E H, Sheppard R J and South G P 1978 *Dielectric behavior of biological molecules* (Oxford: Clarendon)
33. Gregory R B (ed.) 1995 *Protein-solvent interactions* (New York: Marcel Dekker)
34. Pethig R 1992 *Annu. Rev. Phys. Chem.* **43** 177
35. Nandi N and Bagchi B 1997 *J. Phys. Chem.* **B101** 10954
36. Balasubramanian S, Pal S and Bagchi B 2002 *Phys. Rev. Lett.* **89** 115505-1
37. Balasubramanian S and Bagchi B 2001 *J. Phys. Chem.* **B105** 12529
38. Pal S, Balasubramanian S and Bagchi B 2003 *J. Phys. Chem.* **B107** 5194
39. Balasubramanian S and Bagchi B 2002 *J. Phys. Chem.* **B106** 3668
40. Bruce C D, Senapati S, Berkowitz M L, Perera L and Forbes M D E 2002 *J. Phys. Chem.* **B106** 10902
41. Vajda S, Jimenez R, Rosenthal S J, Fidler V, Fleming G R and Castner E W Jr 1995 *J. Chem. Soc., Faraday Trans.* **91** 867
42. Sen S, Sukul D, Dutta P and Bhattacharyya K 2001 *J. Phys. Chem.* **A105** 10635
43. Nandi N and Bagchi B 1996 *J. Phys. Chem.* **100** 13914
44. Ju C and Bohnne C 1996 *J. Phys. Chem.* **100** 3847
45. Sen S, Dutta P, Mukherjee S and Bhattacharyya K 2002 *J. Phys. Chem.* **B106** 7745
46. Mandal D, Sen S, Tahara T and Bhattacharyya K 2002 *Chem. Phys. Lett.* **359** 77
47. Sen P, Mukherjee S, Halder A and Bhattacharyya K *Chem. Phys. Lett.* (in press)
48. Venables D S, Huang K and Schmuttenmaer C A 2001 *J. Phys. Chem.* **B105** 9132
49. Dutta P, Sen P, Mukherjee S, Halder A and Bhattacharyya K 2003 *J. Phys. Chem.* **B107** 10815
50. Sen S, Sukul D, Dutta P and Bhattacharyya K 2001 *J. Phys. Chem.* **A105** 7495
51. Faeder J, Albert M V and Ladanyi B M 2003 *Langmuir* **19** 2514
52. Senapati S and Chandra A 2001 *J. Phys. Chem.* **B105** 5106
53. Senapati S and Berkowitz M L 2003 *J. Chem. Phys.* **118** 1937
54. de Gennes P G 1979 in *Scaling concepts in polymer physics* (Ithaca: Cornell University Press)
55. Deo N, Jockusch S, Turro N J and Somasundaran P 2003 *Langmuir* **19** 5083
56. Narenberg R, Kliger J and Horn D 1999 *Angew. Chem., Int. Ed. Engl.* **38** 1626
57. Sen S, Sukul D, Dutta P and Bhattacharyya K 2002 *J. Phys. Chem.* **B106** 3763
58. Dutta P, Sen S, Mukherjee S and Bhattacharyya K 2002 *Chem. Phys. Lett.* **359** 15
59. Dutta P, Sukul D, Sen S and Bhattacharyya K 2003 *Phys. Chem. Chem. Phys.* **5** 4875
60. Lissi E A and Abuin E 1985 *J. Colloid. Inter. Sci.* **105** 1
61. Almgren M, Greiser F and Thomas J K 1979 *J. Am. Chem. Soc.* **101** 279
62. Frauchiger L, Shirota H, Uhrich K E and Castner E W Jr 2002 *J. Phys. Chem.* **B106** 7463
63. Bellissent-Funel M-C (ed.) 1999 *Hydration processes in biology: Theoretical and experimental approaches* (Amsterdam: IOS Press)
64. *Hydration processes in biological and macromolecular systems* 1996 *Faraday Discuss.* **103** p. 1
65. Otting G, Lipenish E and Wuthrich K 1991 *Science* **254** 974
66. Denisov V P, Jonsson B-H and Halle B 1999 *Nature Struct. Biol.* **6** 253
67. Marzola P and Gratton E 1991 *J. Phys. Chem.* **95** 9488
68. Pierce D W and Boxer S G 1992 *J. Phys. Chem.* **96** 5560
69. Jordanides X J, Lang M J, Song X and Fleming G R 1999 *J. Phys. Chem.* **B103** 7995

70. Pal S K, Mandal D, Sukul D, Sen S and Bhattacharyya K 2001 *J. Phys. Chem.* **B105** 1438
71. Dutta P, Sen P, Mukherjee S and Bhattacharyya K 2003 *Chem. Phys. Lett.* **382** 426
72. Pal S K, Peon J and Zewail A H 2002 *Proc. Natl. Acad. Sci. (USA)* **99** 1763
73. Mandal D, Sen S, Sukul D, Bhattacharyya K, Mandal A K, Banerjee R and Roy S 2002 *J. Phys. Chem.* **B106** 10741
74. Pal S K, Peon J and Zewail A H 2002 *Proc. Natl. Acad. Sci. (USA)* **99** 15297
75. Pal S K, Peon J and Zewail A H 2002 *Proc. Natl. Acad. Sci. (USA)* **99** 10964
76. Dutta P, Sen P, Halder A, Mukherjee S, Sen S and Bhattacharyya K 2003 *Chem. Phys. Lett.* **377** 229
77. Sen P, Mukherjee S, Dutta P, Halder A, Mandal D, Banerjee R, Roy S and Bhattacharyya K 2004 *J. Phys. Chem.* **B107** 14563
78. Mukherjee S, Sen P, Halder A, Sen S, Dutta P and Bhattacharyya K 2003 *Chem. Phys. Lett.* **379** 471
79. Brauns E B, Madaras M L, Coleman R S, Murphy C J and Berg M A 2002 *Phys. Rev. Lett.* **88** 158101-1
80. Pal S K, Zhao L, Xia T and Zewail A H 2003 *Proc. Natl. Acad. Sci. (USA)* **100** 13746
81. Farrer R A and Fourkas J T 2003 *Acc. Chem. Res.* **36** 605
82. Pal S K, Sukul D, Mandal D, Sen S and Bhattacharyya K 2000 *J. Phys. Chem.* **B104** 2613
83. Bauman R, Ferrante C, Deeg F W and Brauchle C 2001 *J. Chem. Phys.* **114** 5781
84. Halder A, Sen S, Das Burman, A, Patra A and Bhattacharyya K 2004 *J. Phys. Chem.* (in press)
85. Nag A and Bhattacharyya K 1988 *Chem. Phys. Lett.* **151** 474
86. Nag A and Bhattacharyya K 1989 *Chem. Phys. Lett.* **157** 83
87. Bhattacharyya K and Chowdhury M 1993 *Chem. Rev.* **93** 507
88. Grabowski Z R, Rotkiewicz K and Rettig W 2003 *Chem. Rev.* **103** 3899
89. Fayed T A, Organero J A, Garcia-Ochoa I, Tormo L and Douhal A 2002 *Chem. Phys. Lett.* **364** 108
90. Tolbert L M and Solnsteve K M 2002 *Acc. Chem. Res.* **35** 19
91. Saeki M, Ishiuchi S-I, Sakai M and Fuji M 2001 *J. Phys. Chem.* **A105** 10045
92. Cohen B, Huppert D, Solnsteve K M, Tsfadia Y, Nachliel E and Gutman M 2002 *J. Am. Chem. Soc.* **124** 7539
93. Hansen J E, Pines E and Fleming G R 1992 *J. Phys. Chem.* **96** 6904
94. Mandal, D, Pal S K and Bhattacharyya K 1998 *J. Phys. Chem.* **A102** 9710
95. Dutta P, Halder A, Mukherjee S, Sen P, Sen S and Bhattacharyya K 2002 *Langmuir* **18** 7867
96. Organero J A and Douhal A 2003 *Chem. Phys. Lett.* **373** 426
97. Pal S K, Mandal D, Sukul D and Bhattacharyya K 1999 *Chem. Phys.* **249** 63
98. Tavernier H L, Laine F and Fayer M D 2001 *J. Phys. Chem.* **A105** 8944
99. Kumbhakar M, Nath S and Pal H 2003 *J. Chem. Phys.* **119** 388
100. Chakraborty D, Chakrabarty A, Seth D and Sarkar N 2003 *Chem. Phys. Lett.* **382** 508